Optical technologies applied alongside on-site and remote approaches for climate gas emission quantification at a wastewater treatment plant

Samuelsson, Jerker; Delre, Antonio; Tumlin, Susanne; Hadi, Safa; Offerle, Brian; Scheutz, Charlotte

Published in:
Water Research

Link to article, DOI:
10.1016/j.watres.2017.12.018

Publication date:
2018

Document Version
Peer reviewed version

Accepted Manuscript

Optical technologies applied alongside on-site and remote approaches for climate gas emission quantification at a wastewater treatment plant

Jerker Samuelsson, Antonio Delre, Susanne Tumlin, Safa Hadi, Brian Offerle, Charlotte Scheutz

PII:	S0043-1354(17)31013-8
DOI:	10.1016/j.watres.2017.12.018
Reference:	WR 13416
To appear in:	*Water Research*
Received Date:	19 July 2017
Revised Date:	24 October 2017
Accepted Date:	09 December 2017

Please cite this article as: Jerker Samuelsson, Antonio Delre, Susanne Tumlin, Safa Hadi, Brian Offerle, Charlotte Scheutz, Optical technologies applied alongside on-site and remote approaches for climate gas emission quantification at a wastewater treatment plant, *Water Research* (2017), doi: 10.1016/j.watres.2017.12.018

Optical technologies applied alongside on-site and remote approaches for climate gas emission quantification at a wastewater treatment plant

Jerker Samuelsson [a], Antonio Delre [b], Susanne Tumlin [c], Safa Hadi [c], Brian Offerle [a], Charlotte Scheutz [b]

[a] FluxSense AB, SE-41296 Göteborg, Sweden

[b] Department of Environmental Engineering, Technical University of Denmark, 2800 Kgs. Lyngby, Denmark

[c] Gryaab AB, SE-40274 Göteborg, Sweden

Corresponding author: Charlotte Scheutz

E-mail address: chas@env.dtu.dk

Address: Department of Environmental Engineering, Building 115, Technical University of Denmark, 2800 Kgs. Lyngby, Denmark.

Highlights

- Emissions of CH_4, N_2O, and NH_3 were quantified from a wastewater treatment plant
- Whole-plant and on-site emissions were measured using optical analytical techniques
- Biosolid stockpiles accounted for 70% of total CH_4 emission
- N_2O was principally (about 82%) emitted from nitrifying trickling filters
- Important NH_3 emission sources were biosolid stockpiles and mechanical dewatering

Keywords: Methane, nitrous oxide, ammonia, biosolid stockpiles, sewage sludge, emission factors

Abstract

Plant-integrated and on-site gas emissions were quantified from a Swedish wastewater treatment plant by applying several optical analytical techniques and measurement methods. Plant-integrated CH_4 emission rates, measured using mobile ground-based remote sensing methods, varied between 28.5 and 33.5 kg CH_4 h^{-1}, corresponding to an average emission factor of 5.9% as kg CH_4 (kg CH_4 $_{production}$) $^{-1}$, whereas N_2O emissions varied between 4.0 and 6.4 kg h^{-1}, corresponding to an average emission factor of 1.5% as kg N_2O-N (kg TN $_{influent}$) $^{-1}$. Plant-integrated NH_3 emissions were around 0.4 kg h^{-1}, corresponding to an average emission factor of 0.11% as kg NH_3-N (kg TN $_{removed}$) $^{-1}$. On-site emission measurements showed that the largest proportions of CH_4 (70%) and NH_3 (66%) were emitted from the sludge treatment line (mainly biosolid stockpiles and the thickening and dewatering units), while most of the N_2O (82%) was emitted from nitrifying trickling filters. In addition to being the most important CH_4 source, stockpiles of biosolids exhibited different emissions when the sludge digesters were operated in series compared to in parallel, thus slightly increasing substrate retention time in the digesters. Lower CH_4 emissions and generally higher N_2O and NH_3 emissions were observed when the digesters were operated in series. Loading biosolids onto trucks for off-site treatment generally resulted in higher CH_4, N_2O, and NH_3 emissions from the biosolid stockpiles. On-site CH_4 and N_2O emission quantifications were approximately two-thirds of the plant-integrated emission quantifications, which may be explained by the different timeframes of the approaches and that not all emission sources were identified during on-site investigation. Off-site gas emission quantifications, using ground-based remote sensing methods, thus seem to provide more comprehensive total plant emissions rates, whereas on-site measurements provide insights into emissions from individual sources.

1 Introduction

Wastewater treatment is an anthropogenic source of atmospheric emissions of both methane (CH_4) and nitrous oxide (N_2O). Furthermore, ammonium (NH_4^+) is a compound generated and transformed in biological processes occurring at wastewater treatment plants (WWTPs) (Kampschreur et al., 2009) and could potentially be volatilized as ammonia (NH_3). Methane and N_2O are potent greenhouse gases contributing to climate change (Stocker et al., 2013), which is why their quantifications are important in supporting emission reporting and mitigation. Ammonia is a plant nutrient, and thus emissions in this regards contribute to environmental eutrophication (Jenkinson, 2001). However, quantifying air emissions from WWTPs is a challenging undertaking, as these discharges are diffuse by nature because they emanate from several diverse process units and technologies replete with different physical shapes and emission heights, which, when combined, form a large heterogeneous area source.

In the last 20 years, emission measurements from WWTPs have been performed mainly using on-site point measurement methods. Floating chambers combined with liquid sample analysis have been the most common way of measuring emissions of N_2O and CH_4 from wastewater treatment units with open air basins (Ahn et al., 2010; Czepiel et al., 1995; 1993; Ren et al., 2013; Ye et al., 2014). Lately, long-term investigations have been carried out along different stages of wastewater reactors, in order to shed light on the temporal and spatial variability of emissions (Rodriguez-Caballero et al., 2014; Yan et al., 2014). Although these approaches have increased knowledge about the mechanisms involved in greenhouse gas emissions, they measure only a portion of the emissions from the reactor's surface. A few studies on covered reactors with an air collection system (Daelman et al., 2013; Toyoda et al., 2011) have tried to fill this gap, thereby obtaining a larger dataset with diurnal and annual emission changes. However, this approach can be applied

only to enclosed plants or wastewater treatment units with a ventilation system, and it does not consider physical leakages from pipes and fittings, or any other incidental releases.

In the last few years, ground-based optical remote sensing approaches have also been used for greenhouse gas quantification. The vertical radial plume mapping method, using an open-path gas analyzer, can identify elevated concentrations of CH_4 and N_2O from a wastewater reactor, but this is often limited to quantifying CH_4 emissions only, due to background concentrations of N_2O relative to instrument sensitivity (Modrak et al., 2006). Finally, a highly sensitive mobile analytical platform, applied in conjunction with the tracer dispersion method, has provided plant-integrated greenhouse gas emission rates for several Scandinavian open-air WWTPs, by performance of downwind plume measurements of both CH_4 and N_2O (Yoshida et al., 2014; Delre et al., 2017). Ground-based optical remote sensing methods are considered to provide a more comprehensive overview of whole-site CH_4 emissions from large area sources (Reinelt et al., 2017; Yver Kwok et al., 2015). For ammonia, the scientific literature, to the best knowledge of the authors, does not currently report atmospheric emissions from full-scale urban wastewater treatment plants.

Earlier studies have indicated that greenhouse gas emissions from process units such as biosolid stockpiles and nitrifying trickling filters could be significant (Mønster et al., 2014a; Delre et al. 2017). However, to date, only Majumder et al. (2014) have quantified these emissions from biosolid stockpiles. Air emission process data are important in environmental assessments comparing the environmental performances of different treatment technologies.

This paper aims at presenting for the first time a novel multiple measurement approach for air emission quantifications from a full-scale Swedish WWTP, using several optical analytical technologies and measurement methods, thereby allowing quantifications of air emissions from individual process units as well as the whole plant. Emissions of CH_4, N_2O, and NH_3 were measured, and process parameters, which potentially could influence air emissions, were explored.

Furthermore, we quantified air emissions from biosolid stockpiles and from nitrifying trickling filters used for urban wastewater nitrification. To the best knowledge of the authors NH_3 emissions from various on-site sources as well as plant-integrated emissions have not been measured at a WWTP before.

2 Material and methods

2.1 Site description

The investigated Swedish WWTP treats about 147 Mm^3 wastewater per year, corresponding to a pollution load of about 806,000 population equivalent (PE), 6% of which comes from industry and the rest from households. The facility is divided into three main stages: A mechanical pre-treatment line, a wastewater treatment line, and a sewage sludge treatment line. Incoming pollution is mechanically removed with coarse and fine bar screens, a sand trap, a fat oil and grease trap, and primary settling tanks. The wastewater treatment line is a combination of several process units, starting with a high-loaded activated sludge unit involving pre-denitrification, simultaneous phosphorus precipitation, and biochemical oxygen demand (BOD) removal, followed by secondary settlers. Nitrification is carried out in nitrifying trickling filters, while post-denitrification is performed in moving bed biofilm reactors (MBBRs). Disc filters remove any remaining suspended solids before the treated wastewater is finally discharged into a river. Sewage sludge is thickened before undergoing stabilization through mesophilic anaerobic digestion. Subsequently, the digestate is mechanically dewatered on a centrifuge. Thickening and dewatering operations occur in a building where a ventilation system assures a safe working environment. There is no treatment of the vented air. Centrifuges for dewatering are located in a specific room, separated from the other machines but connected to the same ventilation system. Biosolids obtained after dewatering digested sludge are stored for about three weeks in open-air stockpiles before being transported off-

site. Reject water from the sludge treatment line is recirculated back to the wastewater treatment line. Mechanical and biological treatments are supported, at different stages, through the addition of coagulants and flocculants for phosphorus and solids removal, and methanol for microorganism carbon supply. The plant receives sewage sludge from smaller WWTPs and co-digests industrial food waste. Produced biogas is stored on-site in a gasholder, and routed in pipes to an off-site upgrading facility and used as vehicle fuel. During treatment, sewage sludge can be named differently. Hereafter, the following nomenclature is used to refer to the different treatment stages. After being removed from wastewater, sewage sludge is called "substrate" when entered into the digester. The liquid output of the digestion is called "digestate," which, after increasing its solid content via centrifugation, is called "biosolids". Table 1 provides an overview of key plant-specific information related to the measurement year 2015.

Over 2015, the digesters were run in two different modes: In parallel and in series. Usually, digesters work in parallel with a volatile solids (VS) load of 2.4 kg VS m^{-3} day^{-1}. From June until August, the serial mode was employed, resulting in a sludge retention time of 22 days instead of 20 days. When running in series, the VS load into the first digester increased to 4.4 kg VS m^{-3} day^{-1}, while the second digester had an average load of 2.2 kg VS m^{-3} day^{-1}.

2.2 Optical analytical techniques applied

Several optical analytical technologies were used to detect different compound concentrations in real time: A Fourier transform infrared spectroscopy analyzer (FTIR), for measuring concentrations of C_2H_2, N_2O, CH_4, NH_3, and C_2H_4, and two cavity ring down spectroscopy (CRDS) analyzers, for measuring C_2H_2, N_2O, and CH_4. Table 2 summarizes details regarding the analytical technologies applied for gas concentration measurements.

The FTIR instrument consists of an infrared spectrometer (Bruker Optics GmbH, Matrix-M IRCube) connected to a closed long-path sample cell (Infrared Analysis Inc., model 107-V).

Compound-specific concentrations were determined by infrared absorption spectroscopy, whereby CH_4, N_2O, NH_3, C_2H_4, and C_2H_2 were measured simultaneously and analyzed at 3.3, 4.5, 10.3, 10.5, and 13.7 μm wavelengths, respectively. In mobile mode, the FTIR analyzer logged every ninth second at a precision of 1.7, 0.3, 2.0, 1.8, and 4.7 ppb for CH_4, N_2O, NH_3, C_2H_2, and C_2H_4, respectively (C_2H_2 and C_2H_4 were used as dispersion tracer gases). More information about the instrument can be found in Galle et al. (2001) and Scheutz et al., (2011), and about the FTIR technology in general in the USA Environmental Protection Agency Handbook (Mikel and Merrill, 2011).

CRDS uses an optical technology in which gas concentration is obtained by measuring directly the "ring-down," or decay, of laser light in a sample cell. One instrument was equipped with lasers detecting CH_4 and C_2H_2 (G2203, Picarro, Inc., Santa Clara, CA), and another was set up to identify N_2O and C_2H_2 (S/N JADS2001, Picarro, Inc., Santa Clara, CA). The CH_4/C_2H_2 analyzer logged twice per second with a precision of 0.77 ppb and 0.06 ppb for CH_4 and C_2H_2, respectively. The N_2O/C_2H_2 analyzer recorded every 3 seconds with a precision of 7.7 ppb and 0.6 ppb for N_2O and C_2H_2, respectively. More detailed instrument descriptions can be found in Mønster et al. (2014b) and Yoshida et al. (2014).

2.3 Measurement methods applied

Gas concentration detection, using different optical analytical techniques, was combined with different measurement methods to obtain the emission rate of the target compounds.

Emission rates were obtained mainly by applying the tracer gas dispersion method (TDM), which is based on the principle that gases (with long atmospheric lifetime) disperse in the same way as far as mixing and transport are concerned. Therefore, when good mixing between the two gases is assured, the real-time emission rate of the target gas can be obtained from the relationship between the downwind concentrations of the target gas and the tracer gas. The tracer gas is

167 constantly released from the emitting source and the emission rate is calculated as shown by Eq. 1.
168 In this study, acetylene (C_2H_2) was used as main tracer gas, and ethylene (C_2H_4) was occasionally
169 used as a second tracer to pinpoint a specific source (nitrifying trickling filter).

170 $$E_g = Q_t \frac{(C_g - C_{g\,background})MW_g}{(C_t - C_{t\,background})\,MW_t} \qquad \text{(Eq. 1)}$$

171 E_g is the target gas emission in mass per time; Q_t is the tracer release in mass per time; C_g and C_t
172 are the measured off-gas concentrations in parts per billion (ppb); $C_{g\,background}$ and $C_{t\,background}$
173 are the background concentrations of the target gas and tracer (ppb); and MW_g and MW_t are the
174 molar weights of target gas and tracer gas, respectively (Scheutz et al., 2011). The method can be
175 applied in static or mobile mode. In this study, the static tracer dispersion method was applied at a
176 ventilated duct in the thickening and dewatering building. In this case, C_2H_2 was released upstream
177 in the enclosed ventilation duct, prior to a fan passage, so that proper mixing of tracer and target
178 gases was assured from the gas release point to the concentration sampling point. During
179 measurement, the analytical platform was positioned at a fixed location, and so the mode of the
180 tracer dispersion method is referred to as "static" (STDM). A detailed description of the static mode
181 can be found in Fredenslund et al. (2010). Conversely, the mobile mode of the method relies on
182 dynamic downwind concentration measurements of the mixed target and tracer gases, performed
183 across the plume by using the analytical platform in mobile mode. Concentrations in the mobile
184 mode in this study were integrated over the plume's cross-section to minimize the effects of any
185 improper source simulation and gas mixing (Mønster et al., 2014b). Moreover, in this study, the
186 mobile approach was applied for specific on-site sources and to the whole WWTP for plant-
187 integrated measurements (Table 3). Figure 1 shows an example of downwind plumes used for plant-
188 integrated quantifications. A detailed description of the mobile mode (MTDM) can be found in
189 Yoshida et al. (2014) and Delre et al. (2017).

In the tracer dispersion method's mobile mode, concentration sampling is done at a distance away from the source, and the source emission is inherently dispersed to lower concentration levels substantially at the sampling point compared to nearby the source. Despite the high sensitivity of the analytical instrument used, in cases where the emission rate of one of the target gases is very low, the corresponding downwind plume cannot be properly distinguished from the background concentration when measurements are performed at a long distance to the source. In this case, the emission rate of the less abundant target gas can instead be inferred from the concentration ratio of the less abundant gas to the more abundant target gas as being sampled closer to the source where concentrations are higher, combined with the emission rate of the more abundant target gas as established with the MTDM (see Eq. 2). When measuring the target gas close to the source, care must be taken not to prejudice the ratio, in case the target gases are not homogeneously mixed, and the ratio should be based on an average sampling extended in both space and time.

$$\hat{E}^{i} = \overline{E}^{j} \cdot \frac{1}{k}\sum_{k}\int_{t1}^{t2}\frac{(c_g{}^{i} - c_{g\,background}{}^{i}) \cdot MW_g^{i}}{(c_g{}^{j} - c_{g\,background}{}^{j}) \cdot MW_g^{j}}dt \qquad \text{Eq. 2.}$$

where:

$\hat{E}^{i}$ = the inferred emission rate of the secondary (less abundant) target gas species *i*

$\overline{E}^{j}$ = the average emission rate of the main (more abundant) target gas species *j* obtained from multiple plume transects as measured by MTDM,

$c_g^{i,j}$ = measured off-gas concentration (ppbv) of the main target gas *j* or the secondary target gas *i*,

$c_{g\,background}^{\;\;i,j}$ = measured background concentration (ppbv) of the main target gas *j* or the secondary target gas *i*,

k = the number of gas ratio measurements, each integrated over a time window t_1 to t_2

$MW_g^{i,j}$ = molar weights of the measured main target gas *j* or the secondary target gas *i*,

For gaseous ammonia, the TDM method was complemented by measurements made with the optical remote sensing solar occultation flux (SOF) method (Johansson et al. 2014; Mellqvist et al. 2010, 1999; Mikel and Merrill, 2011). In this study, SOF was used for plant-integrated NH_3 quantification. In Europe, the SOF technique is considered best available technology (BAT) (Brinkmann et al., 2016) for measurements of diffuse emissions of volatile organic compounds (VOCs) in the chemical sector. Recently, the SOF method has been used for NH_3 fugitive emissions characterization from agricultural sources (Kille et al., 2017).

The SOF system applied herein is based on an identical FTIR spectrometer previously described for the TDM method, but instead of an internal infrared source (glowbar), it uses infrared radiation from the sun. Solar light is continuously directed into the FTIR spectrometer by means of a solar tracker as the measurement vehicle moves through the cross-section of the source emission plume, and infrared spectra are then recorded sequentially. The spectra are analyzed for infrared absorption by molecular species present in the source emission plume. The principle for retrieving the target gas emission rate from a source via SOF measurement is given in Eq. 3.

$$E_g = \int_{Plume\ start}^{Plume\ stop}\left(\int_0^{Plume\ top} c_g(z)\cdot u'(z)\cdot dz\right)\cdot dx = \overline{u'_{mass}}\cdot\int_{Plume\ start}^{Plume\ stop} column(x)\cdot dx$$

Eq. 3

where

E_g = emission rate of the target gas

$c_g(z)$ = concentration of the target gas at height (z) above the ground

$u'(z)$ = wind speed at height (z) above the ground, specifically the wind speed component orthogonal to the horizontal travel direction (x) through the plume

$\overline{u'_{mass}}$ = plume mass weighted average wind speed, the component orthogonal to the travel direction (x)

235 $column\ (x)$ = concentration integrated in the vertical through the plume (e.g. along the slant beam
236 of the sun, compensated with a cosine factor of the solar zenith angle).

237 To obtain gas emissions from a target source, the SOF instrument vehicle is driven crosswind
238 through the plume of the source, so that solar light cuts through the plume and vertically integrated
239 gas concentration columns are recorded. The measurement starts with an atmospheric background
240 spectrum sampled outside the source plume, and consecutive spectra are then analyzed by reference
241 to the atmospheric background spectrum. By adding consecutive gas column measurements, the
242 integrated mass of the target species across the source plume is hence obtained. The source flux is
243 retrieved by multiplying the integrated plume mass with the average wind speed of the plume.

244 The FTIR instrument was operated at 0.5 cm^{-1} wavenumber resolution and a 5-second time
245 resolution. Precision in the measured NH_3 column was 0.08 mg/m^2. A prop and vane wind monitor
246 (R.M. Young Wind Monitor, model 05103), mounted on a 4-meter mast at the measurement site,
247 measured wind speed and direction. Wind direction and speed were averaged over 1 minute and
248 recorded by a data logger (Campbell Scientific model CR200). The wind monitor had a stated
249 accuracy of ±3° and ±0.3 ms^{-1}. Uncertainty in the flux estimate obtained by the SOF method was
250 dominated by uncertainty in the wind field (e.g. vertical plume distribution and plume transport
251 speed) and was typically ±30%.

252 **2.4 Measurement campaigns**

253 In total, 13 measurement campaigns spread over three seasons in 2015 were performed under
254 normal plant operations. Table 3 provides an overview of these campaigns, including measurement
255 date and time intervals, applied measurement methods, adopted optical techniques, and target gases.
256

3 Results and discussion

3.1 Plant-integrated emission quantification

During the night between August 28th and 29th, plant-integrated measurements were performed by applying MTDM, with two different analytical platforms (FTIR and CRDS) detecting CH_4, N_2O, and NH_3 (Table 3). Three C_2H_2 gas cylinders, each with a different flow rate, were used to simulate CH_4 emissions from the whole facility. Although part of the CH_4 was emitted from the activated sludge reactors, the dominant CH_4 source was the sludge treatment line. CH_4 emission rates from the two analytical platforms provided comparable results: 28.5 ± 3.1 kg CH_4 h^{-1} and 33.5 ± 3.0 kg CH_4 h^{-1} for FTIR and CRDS, respectively (Table 4). Values are expressed as the average and standard deviations of transects performed (AV ± SD). Figure 2 shows the time series of the plant-integrated CH_4 emission quantification. CH_4 emission rates varied between 38.8 kg CH_4 h^{-1} and 23.4 kg CH_4 h^{-1}, and they did not show any specific release trend throughout the 4 hours of measurements. No unusual operation was reported during the measurement campaign, such as activation of the plant flare system for surplus biogas combustion or emergency venting of the digesters, which may have influenced emission patterns (Reinelt et al., 2015; Yoshida et al., 2014). By normalizing emission rates to plant operation parameters so-called emission factors are obtained, which are used for plant and technology intercomparison accounting for differences in material throughput and process efficiencies. Furthermore, emission factors are often applied for estimation of plant emissions (by multiplying with plant specific parameters e.g. material input or removal efficiencies). Emission reporting based on emission factors is common (e.g. Doorn et al., 2006; Kampschreur et al., 2009) and there is a great need for providing reliable emission factors representing current technologies to improve emission reporting. Table 5 reports CH_4 emissions normalized by CH_4 production from anaerobic sludge digestion (e.g. kg CH_4 emitted per kg CH_4 produced) and by organic load (chemical oxygen demand COD) to the plant (e.g. kg CH_4 emitted

per kg $COD_{influent}$ into the plant), thereby providing CH_4 losses for analysis from an energetic or a treatment capacity perspective, respectively. Since CH_4 was mainly emitted from the sludge treatment, the measured CH_4 emissions were normalized using average CH_4 production and $COD_{influent}$ into the plant recorded during the two months prior to the measurement campaign, in order to account for the plant retention time of carbon entering the plant as COD in the influent and being emitted as CH_4 from the biosolid stockpiles. CH_4 production is recorded every minute whereas the COD in the plant inlet is measured five times per week. EFs were about 5.9% as kg CH_4 (kg CH_4 prod.)$^{-1}$ and about 0.7% as kg CH_4 (kg COD influent)$^{-1}$, using an average whole site CH_4 emission of 31.0 ± 3.1 kg CH_4 h^{-1} (Table 5). Comparing these results with the previous two studies performing plant-integrated CH_4 emission quantification from a Scandinavian WWTP (Yoshida et al., 2014; Delre et al., 2017), CH_4 EF falls into the lower-to-medium part of the reported range (1.1 - 32.7% as kg CH_4 (kg CH_4 prod.)$^{-1}$ and 0.2 - 9.1% as kg CH_4 (kg COD influent)$^{-1}$).

To measure N_2O emissions from the whole facility, one C_2H_2 tracer gas cylinder and one C_2H_4 gas cylinder were placed by the nitrifying trickling filters, as these were by far the most significant N_2O source at the plant. Also for this target gas, the two analytical platforms provided a comparable result: 4.0 ± 0.8 kg N_2O h^{-1} and 6.4 ± 2.1 kg N_2O h^{-1} for FTIR and CRDS, respectively (Table 4). Figure 3 shows the time series of the plant-integrated N_2O emission quantifications, which varied between 2.4 kg N_2O h^{-1} and 11.8 kg N_2O h^{-1}, and no clear trend in the emission was observed. Figure 3 also shows variation in inlet wastewater flowing into the nitrifying trickling filters, as well as the influent of nitrate (NO_3^-) and NH_4^+, albeit no correlation with the measured plant-integrated N_2O emissions could be seen. Similarly, no correlation of plant-integrated N_2O emissions was found either with the drop in NO_3^- formation in the first hour of measurements or with the peaks of NH_4^+ removal occurring during nitrification at the nitrifying trickling filters

(Figure 4). N_2O emissions were normalized according to total nitrogen (TN) loaded into the plant (kg N_2O-N (kg TN influent)$^{-1}$) and to TN removed from the plant (kg N_2O-N (kg TN removed)$^{-1}$). The measured N_2O emission was normalized using the average TN influent and the average TN removed recorded during the week prior to the measurement campaign, to account for the plant retention time of nitrogen entering the plant with the influent and being emitted as N_2O from the nitrifying trickling filters. This was done as the nitrifying trickling filters were found to be main N_2O emission source. No daily variation in TN influent into the plant was considered, as the WWTP only records this data on a weekly basis. The reject water flow made up 2% of the total wastewater flow treated in the nitrifying trickling filters. It was not possible to relate the measured N_2O emissions to the treatment of nitrogen in the reject water as the nitrogen content in the reject water was not measured during the measurement campaign. Only nitrogen in the combined inlet flow to the nitrifying trickling filters (reject water mixed into the main water flow) was measured (as shown in Figure 3 - NO_3^- and NH_4^+ influent flow). On average, the two analytical platforms provided an EF of 0.9% as kg N_2O-N (kg TN influent)$^{-1}$ and an EF equal to 1.2% as kg N_2O-N (kg TN removed)$^{-1}$ (Table 5) when using an average whole-site N_2O emission of 5.2 ± 1.5 kg N_2O h^{-1}. These EFs fall somehow in the middle-lower part of the range (0.1 – 5.2% as kg N_2O-N (kg TN influent)$^{-1}$ and 0.1 – 5.9% as kg N_2O-N (kg TN removed)$^{-1}$)—as reported by previous plant-integrated N_2O emission quantifications of Scandinavian WWTPs (Yoshida et al., 2014; Delre et al., 2017).

Plant-integrated NH_3 measurements were performed in two different campaigns using two different measurement methods but the same optical analytical technology, namely MTDM and SOF, with both using FTIR (Table 3). The main NH_3 source was the sludge treatment line. On July 2nd, SOF measurements provided emissions of 0.4 ± 0.1 kg NH_3 h^{-1}, which were similar to

328 measurements performed with MTDM during the night between August 28th and 29th and resulting
329 in an emission of 0.4 ± 0.2 kg NH_3 h^{-1} (Table 4).

330 Figure 5 shows plant-integrated NH_3 emission rates over time, recorded in the August
331 campaign, which varied between 0.24 kg NH_3 h^{-1} and 0.67 kg NH_3 h^{-1}, with two peak emissions
332 measured around 00:30 and 02:00 (August 28th and 29th). The main NH_3-emitting units were
333 biosolid stockpiles and thickening and dewatering buildings. Figure 5 shows no correlation between
334 the recorded peaks of plant-integrated NH_3 emissions and variation in the flow of digestate to the
335 centrifuges, or the flow of biosolids to the stockpiles. After almost one hour of measurements on
336 July 2nd, plant-integrated NH_3 emission quantifications did not show any trend (results not shown).
337 Considering the different nitrogen species in the wastewater and the strict relationship between NH_3
338 and NH_4^+, NH_3 emissions were normalized not only with TN influent and TN removed to and from
339 the plant, but also with NH_4^+ influent and NH_4^+ removed (Table 5). The measured NH_3 emission
340 was normalized using the average TN influent and TN removed recorded during the two months
341 prior to the measurement campaign, in order to account for the plant retention time of nitrogen
342 entering the plant and being emitted as NH_3 from the biosolid stockpiles. This was done because
343 sludge treatment processes (sludge dewatering and biosolid storage) were found to be the most
344 important NH_3 emission sources. NH_3 EFs were 0.09% as kg NH_3-N (kg $TN_{influent}$)$^{-1}$, 0.11% as kg
345 NH_3-N (kg $TN_{removed}$)$^{-1}$, 0.12% as kg NH_3-N (kg $NH_4^+{}_{influent}$)$^{-1}$, and 0.15% as kg NH_3-N (kg NH_4^+
346 $_{removed}$)$^{-1}$ (Table 5). Since this is the first time that NH_3 air emissions have been quantified from a
347 full-scale WWTP, no literature comparison is possible.
348

3.2 On-Site emission quantifications

3.2.1 On-site CH_4 emission sources and rates

Table 4 reports emission rates for all on-site CH_4 emitting process units, while Figure 6 provides the average contribution of each process unit to the total CH_4 emission quantified from on-site sources. For each process unit, the average emission rate (Figure 6) was calculated based on emission rates obtained in the different measurement campaigns (Table 4). The average emission value for the biosolid stockpiles was calculated as a weighted value according to the operation of digesters, namely in parallel and serial modes. The most important on-site CH_4 sources included the biosolid stockpiles (70%), ventilation from the thickening and dewatering building (11%), the sand trap inlet (9%), and the activated sludge reactors (5%) (Figure 6). Overall, about 81% of the CH_4 emission quantified on-site was released from the sludge treatment line.

Figure 7 shows CH_4 emissions from the biosolid stockpiles normalized by the amount of stored material. CH_4 emissions from still stockpiles were quantified over five measurement campaigns, the first two of which were performed in winter when biosolids were produced with digesters operated in the parallel mode, while the last three measurement campaigns were performed in summer when the biosolids were produced with digesters operated in the serial mode. In the first two summer campaigns, measurements were performed when stockpiles were still and during truck loading of biosolids for off-site treatment. Higher emissions were obtained from biosolids produced when the digesters were operated in parallel (on average $8.77 \cdot 10^{-6}$ kg CH_4 (kg TS biosolids)$^{-1}$ h^{-1}) in comparison to when they were operated in the series mode (on average $3.77 \cdot 10^{-6}$ kg CH_4 (kg TS biosolids)$^{-1}$ h^{-1}). The lower CH_4 emission obtained when operating the digesters in series mode was most likely a result of the higher share of input sludge CH_4 potential being realized as the retention time for a larger share of the substrate in the digesters increased. In fact, the CH_4 production was 7% higher when operating the reactors in series mode, in comparison

to when operated in parallel. A comparison of emissions escaping from still stockpiles and during truck loading showed a CH_4 release about 1.5-2.2 times higher as soon as the piles were moved during loading. We suspect the higher release during loading to be caused by stripping of CH_4 locked up in the sludge pore space or dissolved in the liquid phase of the sludge.

The second most important CH_4 source was the ventilation exhaust of the thickening and dewatering building, which resulted in an average release of 2.3 kg CH_4 h^{-1} and represented 11% of the total CH_4 emissions measured from on-site sources.

CH_4 stripping from the sand trap inlet resulted in an average release of 1.8 kg CH_4 h^{-1} (or about 9% of total CH_4 emissions). Activated sludge reactors covered about 5% of the total CH_4 emission quantified on-site with an average release of 1 kg CH_4 h^{-1}. Primary and secondary settling tanks covered about 4% and 2% of the total CH_4 emissions quantified on-site with an average release of 0.8 and 0.4 kg CH_4 h^{-1}, respectively. Less than 1% of the total CH_4 emissions quantified on-site was provided by nitrifying trickling filters and post-denitrifying MBBR tanks.

The sum of the emission for the on-site sources was 20.8 kg CH_4 h^{-1}. Although measurements were not performed at the same time, a qualitative comparison between on-site and off-site measurements showed that the on-site CH_4 emission rate was about two-thirds of the plant-integrated CH_4 emission quantification (on average about 31.0 kg CH_4 h^{-1}). The lower emission rate obtained by measuring individual on-site sources in comparison to the plant-integrated emission, apart from different timeframes, was most likely a result of not identifying all on-site sources. In this study, potential missing sources could be CH_4 slippages from the sludge treatment line and other unknown sources. Previous studies have reported significant CH_4 losses from the sludge treatment line (Yoshida et al., 2014; Delre et al. 2017), underlining the reasonably higher value of plant-integrated emission rates than on-site measurements, because the former decrease the risk of

missing important emission sources at the facility (Jensen et al., 2017; Reinelt et al., 2017; Yver Kwok et al., 2015).

Furthermore, other studies that have included an investigation of both wastewater and sewage sludge lines have reported that the largest part of the CH_4 emitted from WWTPs is lost from the sludge treatment line (Daelman et al., 2012; Delre et al., 2017). Both Mønster et al. (2014a) and Delre et al. (2017) cited biosolid stockpiles as an important CH_4 source in WWTPs, but they reported only plant-integrated measurements. Conversely, Majumder et al. (2014) investigated seasonal CH_4 emissions from large biosolid stockpiles produced at a WWTP in Australia. Using a closed static chamber method, emissions were measured from stockpiles of different ages: More than 3 years old, 1-3 years old, and less than 1 year old. CH_4 emissions measured from the less than 1-year old biosolid stockpiles were about $8.15 \cdot 10^{-10}$ kg CH_4 (kg TS biosolids)$^{-1}$ h^{-1}, which is lower than the biosolids CH_4 emissions measured in our study (which varied between $1.68 \cdot 10^{-6}$ and $9.29 \cdot 10^{-6}$ kg CH_4 (kg TS biosolids)$^{-1}$ h^{-1} (Figure 7)). The higher emissions measured in our study are most likely a result of the shorter storage time (about 3 weeks) in comparison to those in Majumder et al. (2014) (less than one year). Larsen et al. (2017) measured CH_4 emissions from biosolid stockpiles of mechanical dewatered sludge and reported emissions of $1.98 \cdot 10^{-5}$ kg CH_4 (kg TS biosolids)$^{-1}$ h^{-1}, which were measured from mechanical dewatered surplus activated sludge (less than one week old) that had not been stabilized by anaerobic digestion prior to dewatering, thus potentially explaining the relatively high emission rates. Our emission rates are important for plant emission reporting while for environmental assessment the emissions from off-site long-term sludge storage should also be considered. In Scandinavia, the sludge storage time could be up to about 6 months as sludge is most often applied in spring and autumn. It is possible that the emission rates reported by Majumder et al. (2014) are more representative for longer-term (up to one year) sludge storage. Larsen et al. (2017) also reports CH_4 emission rates for longer-term (4 months) sludge

storage ($3.55 \cdot 10^{-6}$ kg CH_4 (kg TS biosolids)$^{-1}$ h^{-1}), which are lower than for short-term (less than a one week old) storage of mechanical dewatered sludge. CH_4 emissions from mechanical pre-treatment have been reported (Wang et al., 2011; Yan et al., 2014) and explained as the consequence of CH_4 formation in the sewer network due to anaerobic conditions (Liu et al., 2015).

3.2.2 On-site N_2O emission sources and rates

Table 4 reports emission rates for all N_2O-emitting process units, while Figure 6 shows the average contribution of all process units to the total N_2O emissions quantified from on-site sources. For each process unit, the average emission rate (Figure 6) was calculated based on emission rates obtained in the different measurement campaigns (Table 4).The total on-site N_2O emission quantification (3.3 kg N_2O h^{-1}) was about two-thirds of the plant-integrated emission quantification (5.2 kg N_2O h^{-1}), which was similar to the CH_4 results comparing on-site emissions with total emissions.

The most relevant N_2O emission sources were the nitrifying trickling filters, which emitted about 2.7 kg N_2O h^{-1}, covering about 82% of the total N_2O emission quantified on-site (Figure 6). Secondary settling tanks and biosolid stockpiles each covered about 5% of the total N_2O emissions quantified on-site - each with an average annual release of 0.2 kg N_2O h^{-1}. Figure 7 describes N_2O emissions from biosolids normalized by the amount of material stored. In general, lower N_2O emissions were obtained from the produced biosolids when the digesters were operated in parallel (on average $1.69 \cdot 10^{-8}$ kg N_2O-N (kg TS biosolids)$^{-1}$ h^{-1}), in comparison to when the digesters were operated in the series mode (on average $7.16 \cdot 10^{-8}$ kg N_2O-N (kg TS biosolids)$^{-1}$ h^{-1}). This variation in emissions cannot be explained by variations in concentrations of TS, TN, and NH_4-N in the produced biosolids, as these did not change significantly between the two different digestion modes: Average TN concentrations were 43.7 and 43.5 g (kg TS)$^{-1}$ for the serial and the parallel mode, respectively, while average NH_4-N concentrations were 12.4 and 12.7 g (kg TS)$^{-1}$ for the serial and the parallel mode, respectively (Figure 8). The small change in TS content was caused mainly by

444 the centrifuge's dewatering capabilities. It is possible that higher temperatures during summer in
445 comparison to winter resulted in higher microbial activity and thus caused higher emissions during
446 summer. However, this was not the case for CH_4, as the highest emissions were recorded during
447 winter when the reactors were operated in parallel. During truck loading, N_2O emissions were
448 almost four times higher than from the still piles; however, in July, N_2O emissions during truck
449 loading were comparable to the still piles (Figure 7). Considering the emission of both CH_4 and
450 N_2O, the total greenhouse gas emission from biosolids reported in CO_2-equivalents was lower
451 ($1.35 \cdot 10^{-4}$ kg CO_2 eq. (kg TS biosolids)$^{-1}$ h^{-1}) when the reactors were operated in a serial mode in
452 comparison to a parallel mode ($2.53 \cdot 10^{-4}$ kg CO_2 eq. (kg TS biosolids)$^{-1}$ h^{-1}).

453 Post-denitrifying MBBR, primary settling tanks, activated sludge reactors, the sludge
454 treatment building, and the sand trap inlet had average emission rates lower than 0.1 kg N_2O h^{-1} and
455 collectively made up only a small share (8%) of the total N_2O emission quantified on-site (Figure
456 6).

457 Different N_2O emission rates recorded by different campaigns at nitrifying trickling filters and
458 biosolid stockpiles (Table 4) could be justified by the complex relationship between N_2O generation
459 and different factors such as oxygen availability, nitrite content, COD, and TN ratio (Kampschreur
460 et al., 2009).

461 Majumder et al. (2014) investigated N_2O emissions from large still biosolid stockpiles less
462 than 1 year old and reported their emissions as $1.64 \cdot 10^{-8}$ kg N_2O-N (kg TS biosolids)$^{-1}$ h^{-1}, which is
463 within the range measured in our study (from $3.3 \cdot 10^{-9}$ kg N_2O-N (kg TS biosolids)$^{-1}$ h^{-1} to $1.25 \cdot 10^{-7}$
464 kg N_2O-N (kg TS biosolids)$^{-1}$ h^{-1} (Figure 7)). Similarly, Larsen et al. (2017) measured N_2O
465 emissions escaping from biosolid stockpiles of mechanically dewatered sludge and reported
466 emissions of $1.44 \cdot 10^{-7}$ kg N_2O-N (kg TS biosolids)$^{-1}$ h^{-1} for material less than one week old while

467 the emission rate of older material (stored for 4 months) was $3.97 \cdot 10^{-8}$ kg N_2O-N (kg TS biosolids)$^{-1}$
468 h^{-1}.

469 **3.2.3 On site NH_3 emission sources and rates**

470 Table 4 reports emission rates for all NH_3 emitting process units, while Figure 6 shows the average
471 contribution of all process units to the total NH_3 emission quantified on-site. For each process unit,
472 the average emission rate (Figure 6) was calculated based on emission rates obtained in the different
473 measurement campaigns (Table 4). The most important NH_3-releasing process units were the
474 biosolid stockpiles and the exhaust used to ventilate the thickening and dewatering building,
475 contributing 44% and 22% of the total NH_3 emissions quantified on-site and emitting 0.17 and 0.09
476 kg NH_3 h^{-1}, respectively. Lower NH_3 emissions were in general obtained from biosolids produced
477 when the digesters were operated in parallel (on average $4.87 \cdot 10^{-8}$ kg NH_3-N (kg TS biosolids)$^{-1}$ h^{-1})
478 in comparison to when they were operated in series mode (on average $6.94 \cdot 10^{-8}$ kg NH_3-N (kg TS
479 biosolids)$^{-1}$ h^{-1}). This difference cannot be explained by changes in concentrations of TS, TN, and
480 NH_4-N in the produced biosolids (Figure 8). In the campaign performed in June, NH_3 emissions
481 were almost the same during truck loading and still biosolids (Figure 7), whereas in the July
482 campaign, they emissions were almost three times higher during truck loading in comparison to the
483 still stockpiles (Figure 7).

484 Settling tanks (primary and secondary), the sand trap inlet, activated sludge reactors, and
485 nitrifying trickling filters all contributed to the remaining percentage (34%) of the total NH_3
486 emissions quantified on-site (Figure 6). The sum of the average NH_3 emissions quantified on-site
487 from different process units provided approximately the same emission rate obtained when
488 quantifying plant-integrated NH_3 emissions (0.4 kg NH_3 h^{-1}) (Table 4), although the measurements
489 represent different timeframes.

490

4 Conclusions

- Plant-integrated CH_4 emission rates measured using ground-based remote sensing methods varied between 28.5 and 33.5 kg CH_4 h^{-1}, corresponding to an average emission factor of 5.9% as kg CH_4 (kg $CH_{4\ production}$) $^{-1}$, whereas N_2O emissions varied between 4.0 and 6.4 kg h^{-1}, corresponding to an average emission factor of 0.9% as kg N_2O-N (kg $TN_{\ influent}$) $^{-1}$.
- Plant-integrated NH_3 emissions were around 0.4 kg h^{-1}, corresponding to an average emission factor of 0.11% as kg NH_3-N (kg $TN_{\ removed}$) $^{-1}$.
- On-site measurements showed that the largest proportion of the CH_4 was emitted from the sludge treatment line, with about 70% coming from biosolid stockpiles. While about 82% of the N_2O was emitted from nitrifying trickling filters, the most relevant NH_3 sources were the biosolid stockpiles (44%) and the thickening and dewatering building (22%).
- Biosolids showed different emissions when the sludge digesters were operated in series rather than in parallel mode, as usually done at the WWTP. When the digesters were operated in series mode, lower CH_4 emissions and generally higher N_2O and NH_3 emissions were observed. Emissions of CH_4, N_2O, and NH_3 tended to be higher while loading biosolids onto trucks.
- On-site CH_4 and N_2O emission quantifications accounted for approximately two-thirds of the plant-integrated emission quantifications. The difference could be a combined effect of different survey timeframes and that no sources were identified during the on-site investigation. Off-site air emission quantifications, using ground-based remote sensing methods, thus seem to provide more comprehensive total plant emission rates, whereas on-site measurements provide insights into emissions from individual sources.

References

Ahn, J.H., Kim, S., Park, H., Rahm, B., Pagilla, K., Chandran, K., 2010. N_2O emissions from

activated sludge processes, 2008-2009: results of a national monitoring survey in the United States. Environ. Sci. Technol. 44, 4505–11. doi:10.1021/es903845y

Brinkmann, T., Giner Santonja, G., Yükseler, H., Roudier, S., Delgado Sancho, L., 2016. 2016. Best Available Techniques (BAT) Reference Document for Common Waste Water and Waste Gas Treatment/Management Systems in the Chemical Sector. Industrial Emissions Directive 2010/75/EU (Integrated Pollution Prevention and Control); Publications Office. doi:10.2791/37535

Czepiel, P., Crill, P., Harriss, R., 1995. Nitrous oxide emissions from municipal wastewater treatment. Environ. Sci. Technol. 29, 2352–2356. doi:10.1021/es00009a030

Czepiel, P., Crill, P., Harriss, R., 1993. Methane emissions from municipal wastewater treatment processes. Environ. Sci. Technol. 27, 2472–2477. doi:10.1021/es00048a025

Daelman, M.R.J., van Voorthuizen, E.M., van Dongen, L.G.J.M., Volcke, E.I.P., van Loosdrecht, M.C.M., 2013. Methane and nitrous oxide emissions from municipal wastewater treatment - results from a long-term study. Water Sci. Technol. 67, 2350–2355. doi:10.2166/wst.2013.109

Daelman, M.R.J., van Voorthuizen, E.M., van Dongen, U.G.J.M., Volcke, E.I.P., van Loosdrecht, M.C.M., 2012. Methane emission during municipal wastewater treatment. Water Res. 46, 3657–3670. doi:10.1016/j.watres.2012.04.024

Delre, A., Mønster, J., Scheutz, C., 2017. Greenhouse gas emission quantification from wastewater treatment plants, using a tracer gas dispersion method. Sci. Total Environ. 605–606, 258–268. https://doi.org/10.1016/j.scitotenv.2017.06.177

Doorn, M.R.J., Towprayoon, S., Manso Vieira, S.M., Irving, W., Palmer, C., Pipatti, R., Wang, C., 2006. IPCC 2006, 2006 IPCC Guidelines for National Greenhouse Gas Inventories, Prepared by the National Greenhouse Gas Inventories Programme - Volume 5: Waste. Hayama, Japan.

538 Fredenslund, A.M., Scheutz, C., Kjeldsen, P., 2010. Tracer method to measure landfill gas
539 emissions from leachate collection systems. Waste Manag. 30, 2146–2152.
540 doi:10.1016/j.wasman.2010.03.013

541 Galle, B., Samuelsson, J., Svensson, B.H., Borjesson, G., 2001. Measurements of methane
542 emissions from landfills using a time correlation tracer method based on FTIR absorption
543 spectroscopy. Environ. Sci. Technol. 35, 21–25.

544 Jenkinson, D.S., 2001. The impact of humans on the nitrogen cycle, with focus on temperate arable
545 agriculture. Plant Soil 228, 3–15. doi:10.1023/A:1004870606003

546 Jensen, M.B., Møller, J., Mønster, J., Scheutz, C., 2017. Quantification of greenhouse gas
547 emissions from a biological waste treatment facility. Waste Manag.
548 https://doi.org/10.1016/j.wasman.2017.05.033

549 Johansson, J. k. E., Mellqvist, J., Samuelsson, J., Offerle, B., Lefer, B., Rappenglück, B., Flynn, J.,
550 Yarwood, G., 2014. Emission measurements of alkenes, alkanes, SO_2, and NO_2 from
551 stationary sources in Southeast Texas over a 5 year period using SOF and mobile DOAS. J.
552 Geophys. Res. Atmos. 1973–1991. doi:10.1002/2013JD020485

553 Kampschreur, M.J., Temmink, H., Kleerebezem, R., Jetten, M.S.M., van Loosdrecht, M.C.M.,
554 2009. Nitrous oxide emission during wastewater treatment. Water Res. 43, 4093–4103.
555 doi:10.1016/j.watres.2009.03.001

556 Kille, N., Baidar, S., Handley, P., Ortega, I., Sinreich, R., Cooper, O.R., Hase, F., Hannigan, J.W.,
557 Pfister, G., Volkamer, R., 2017. The CU mobile Solar Occultation Flux instrument: structure
558 functions and emission rates of NH_3, NO_2 and C_2H_6. Atmos. Meas. Tech. 373–392.
559 doi:10.5194/amt-10-373-2017

560 Larsen, J. D., ten Hoeve, M., Nielsen, S., Scheutz, C. 2017. Life cycle assessment comparing the

561 treatment of surplus activated sludge in a sludge treatment reed bed system with mechanical
562 treatment on centrifuge. Submitted to Journal of Cleaner Production, May 2017.

563 Liu, Y., Ni, B.-J., Sharma, K.R., Yuan, Z., 2015. Methane emission from sewers. Sci. Total
564 Environ. 524–525, 40–51. doi:10.1016/j.scitotenv.2015.04.029

565 Majumder, R., Livesley, S.J., Gregory, D., Arndt, S.K., 2014. Biosolid stockpiles are a significant
566 point source for greenhouse gas emissions. J. Environ. Manage. 143, 34–43.
567 doi:10.1016/j.jenvman.2014.04.016

568 Mellqvist, J., 1999. Application of infrared and UV-visible remote sensing techniques for studying
569 the stratosphere and for estimating anthropogenic emissions. PhD; Chalmers tekniska
570 högskola, Göteborg, Sweden. Göteborg, Sweden.

571 Mellqvist, J., Samuelsson, J., Johansson, J., Rivera, C., Lefer, B., Alvarez, S., Jolly, J., 2010.
572 Measurements of industrial emissions of alkenes in Texas using the solar occultation flux
573 method. J. Geophys. Res. 115, 1–13. doi:10.1029/2008JD011682

574 Mikel, D.K., Merrill, R., 2011. EPA Handbook : Optical Remote Sensing for Measurement and
575 Monitoring of Emissions Flux. Research Triangle, North Carolina, 27711.

576 Modrak, M., D'Amato, V., Doorn, M., Hashmonay, R., Vergara, W., Deeb, A., Suarez, C.,
577 Aparicio, C., Cuevas, M., 2006. Characterization of fugitive emissions of greenhouse gases
578 from a wastewater treatment plant using the radial plume mapping technique, in: WEFTEC
579 2006 - Water Environment Federation. Water Environment Foundation, Dallas - Texas, pp.
580 7200–7205.

581 Mønster, J., Gustavsson, D., Scheutz, C., 2014a. Plume measurements for quantifying CH_4 and
582 N_2O emissions from three wastewater treatment plants, in: Canziani, R., Fatone, F., Evangelia,
583 K. (Eds.), ecoSTP2014 - EcoTechnologies for Wastewater Treatment. Verona - Italy, from 23-

584 27 June 2014, pp. 320–323.

585 Mønster, J., Samuelsson, J., Kjeldsen, P., Rella, C.W., Scheutz, C., 2014b. Quantifying methane
586 emission from fugitive sources by combining tracer release and downwind measurements - a
587 sensitivity analysis based on multiple field surveys. Waste Manag. 34, 1416–1428.
588 doi:10.1016/j.wasman.2014.03.025

589 Reinelt, T., Delre, A., Westerkamp, T., Holmgren, M.A., Liebetrau, J., Scheutz, C., 2017.
590 Comparative use of different emission measurement approaches to determine methane
591 emissions from a biogas plant. Waste Manag. in press.

592 Reinelt, T., Liebetrau, J., Nelles, M., Biomasseforschungszentrum, D., 2015. Operational methane
593 emissions from pressure relief vents on two agricultural biogas plants, in: International
594 Conference on Solid Waste. Hong Kong.

595 Ren, Y.G., Wang, J.H., Li, H.F., Zhang, J., Qi, P.Y., Hu, Z., 2013. Nitrous oxide and methane
596 emissions from different treatment processes in full-scale municipal wastewater treatment
597 plants. Environ. Technol. 34, 2917–2927. doi:10.1080/09593330.2012.696717

598 Rodriguez-Caballero, A., Aymerich, I., Poch, M., Pijuan, M., 2014. Evaluation of process
599 conditions triggering emissions of green-house gases from a biological wastewater treatment
600 system. Sci. Total Environ. 493, 384–391. doi:10.1016/j.scitotenv.2014.06.015

601 Scheutz, C., Samuelsson, J., Fredenslund, a M., Kjeldsen, P., 2011. Quantification of multiple
602 methane emission sources at landfills using a double tracer technique. Waste Manag. 31,
603 1009–1017. doi:10.1016/j.wasman.2011.01.015

604 Stocker, T.F., Qin, D., Plattner, G.-K., Tignor, M., Allen, S.K., Boschung, J., Nauels, A., Xia, Y.,
605 Bex, V., Midgley, P.M., (eds.), 2013. IPCC, 2013: Climate Change 2013: The Physical
606 Science Basis. Contribution of Working Group I to the Fifth Assessment Report of the

607 Intergovernmental Panel on Climate Change. Cambridge, United Kingdom.

608 Toyoda, S., Suzuki, Y., Hattori, S., Yamada, K., Fujii, A., Yoshida, N., Kouno, R., Murayama, K.,
609 Shiomi, H., 2011. Isotopomer analysis of production and consumption mechanisms of N_2O
610 and CH_4 in an advanced wastewater treatment system. Environ. Sci. Technol. 45, 917–922.
611 doi:10.1021/es102985u

612 Wang, J., Zhang, J., Xie, H., Qi, P., Ren, Y., Hu, Z., 2011. Methane emissions from a full-scale
613 A/A/O wastewater treatment plant. Bioresour. Technol. 102, 5479–5485.
614 doi:10.1016/j.biortech.2010.10.090

615 Yan, X., Li, L., Liu, J., 2014. Characteristics of greenhouse gas emission in three full-scale
616 wastewater treatment processes. J. Environ. Sci. 26, 256–263. doi:10.1016/S1001-
617 0742(13)60429-5

618 Ye, L., Ni, B.-J., Law, Y., Byers, C., Yuan, Z., 2014. A novel methodology to quantify nitrous
619 oxide emissions from full-scale wastewater treatment systems with surface aerators. Water
620 Res. 48, 257–68. doi:10.1016/j.watres.2013.09.037

621 Yoshida, H., Mønster, J., Scheutz, C., 2014. Plant-integrated measurement of greenhouse gas
622 emissions from a municipal wastewater treatment plant. Water Res. 61, 108–118.
623 doi:10.1016/j.watres.2014.05.014

624 Yver Kwok, C.E., Müller, D., Caldow, C., Lebègue, B., Mønster, J.G., Rella, C.W., Scheutz, C.,
625 Schmidt, M., Ramonet, M., Warneke, T., Broquet, G., Ciais, P., 2015. Methane emission
626 estimates using chamber and tracer release experiments for a municipal waste water treatment
627 plant. Atmos. Meas. Tech. 8, 2853–2867. doi:10.5194/amt-8-2853-2015

628

629

630 **TABLES**

631 Table 1. Plant key parameters in the investigated year.

Year		2015
Population Equivalent (PE)		805,000
Treated wastewater (m^3 yr^{-1})		147,300,000
Influent wastewater (Mg yr^{-1})	BOD	20555
	COD	43431
	TN	3366
	NH_4^+-N	2367
Effluent (Mg yr^{-1})	BOD	1150
	COD	5916
	TN	1169
	NH_4^+-N	823
Pollutant removal (%)	BOD	94.4
	COD	86.4
	TN	65.3
	NH_4^+-N	65.2
External material treated at the plant (Mg yr^{-1})	Food waste	13,783
	Sewage sludge	79,220
Plant production	Biosolids (Mg TS yr^{-1})	14,846
	Biogas (m^3 yr^{-1})	11,496,818
	CH_4 content in biogas (%)	63.1

633 Table 2. Overview of applied optical analytical techniques.

Optical technique	Measuring principle	Model	Measured gas	Used absorption wave length	Precision	Detection frequency
FTIR	Infrared absorption spectroscopy	IRCube Matrix-M, Bruker Optics GmbH, Ettlingen, Germany	CH_4	3.3 µm	1.7 ppb	9 s
			N_2O	4.5 µm	0.3 ppb	9 s
			NH_3	10.3 µm	2.0 ppb (MTDM) 0.08 mg/m^2 (SOF)	9 s (MTDM) 5 s (SOF)
			C_2H_2	13.7 µm	1.8 ppb	9 s
			C_2H_4	10.5 µm	4.7 ppb	9 s
CRDS	Gas concentration is obtained by measuring directly the "ring-down," or decay of laser light in a sample cell.	G2203, Picarro, Inc., Santa Clara, CA	CH_4	NA	0.77 ppb	0.5 s
			C_2H_2	NA	0.06 ppb	
		S/N JADS2001, Picarro, Inc., Santa Clara, CA	N_2O	NA	7.7 ppb	3 s
			C_2H_2	NA	0.6 ppb	

634 FTIR: Fourier Transform Infrared. CRDS: Cavity Ring-Down Spectroscopy. NA: Information not available. Precision: the capability to reproduce the same
635 concentration measurement and is expressed as the standard deviation of concentrations recorded during a specific time frame (FTIR: 10 minutes, CRDS: 60 minutes)
636 when a gas with a constant concentration goes through the instrument.

637 Table 3. Overview of performed measurement campaigns in 2015.

Date (dd/mm)	Campaign starting time (hh:mm)	Campaign ending time (hh:mm)	Waste water treatment process unit investigated	Optical analytical technology applied	Investigated emissions and measuring method (as superscript, STDM [1], MTDM [2], SOF [3], inferred flux [4] using STDM, MTDM, or SOF of main target gas combined with mass ratio measurement of the less abundant gas in plume versus the main target gas)
12/01	11:28	14:40	Ventilation exhaust of thickening and dewatering building	FTIR	N_2O [1], CH_4 [1], NH_3 [1]
13/01	12:26	13:48	Biosolid stockpiles	FTIR	CH_4 [2], N_2O [4], NH_3 [4]
	14:24	14:48	Primary settlers	FTIR	CH_4 [2], N_2O [4], NH_3 [4]
14/01	11:45	12:03	Biosolid stockpiles	FTIR	CH_4 [2], N_2O [4], NH_3 [4]
	13:47	14:45	Sand trap inlet	FTIR	N_2O [2], CH_4 [2], NH_3 [2]
19/02	13:19	14:19	Nitrifying trickling filters	FTIR	N_2O [2]
	13:18	14:19	Post-denitrifying MBBR	FTIR	N_2O [2], CH_4 [4], NH_3 [4]
	13:17	14:14	Secondary settlers	FTIR	N_2O [2], CH_4 [2], NH_3 [2]
09/03	11:39	12:13	Nitrifying trickling filters	FTIR	N_2O [2], CH_4 [4], NH_3 [4]
11/03	10:53	11:58	Sand trap inlet	FTIR	N_2O [2], CH_4 [2], NH_3 [2]
	11:05	13:15	Primary settlers	FTIR	CH_4 [2], N_2O [4], NH_3 [4]
17/06	10:24	11:16	Ventilation exhaust of thickening and dewatering building	FTIR	N_2O [1], CH_4 [1], NH_3 [1]
	11:54	12:15	Centrifuge room	FTIR	N_2O [1], CH_4 [1], NH_3 [1]
23/06	10:37	12:25	Nitrifying trickling filters	FTIR	N_2O [2]
	13:30	14:22	Activated sludge reactors	FTIR	CH_4 [2], N_2O [4], NH_3 [4]
24/06	10:21	13:01	Biosolid stockpiles	FTIR	CH_4 [2], N_2O [4], NH_3 [4]
02/07	10:45	11:37	Whole plant (plant-integrated measurements)	FTIR	NH_3 [3]
06/07	11:42	14:52	Biosolid stockpiles	FTIR	CH_4 [2], N_2O [4], NH_3 [4]
28/08	23:18	23:32	Ventilation exhaust of thickening and dewatering building	FTIR	CH_4 [2]
28&29/08	23:51	00:44	Nitrifying trickling filters	FTIR	N_2O [2]
	23:22	00:58	Biosolid stockpiles	FTIR	CH_4 [2], N_2O [4], NH_3 [4]
	22:30	02:30	Whole plant (plant-integrated measurements)	FTIR	N_2O [2], CH_4 [2], NH_3 [2]
				CRDS	N_2O [2], CH_4 [2]

638 MTDM: Mobile Tracer Dispersion Method. STDM: Static Tracer Dispersion Method. SOF: Solar Occultation Flux. FTIR: Fourier Transform Infrared. CRDS: Cavity
639 Ring-Down Spectroscopy. MBBR: Moving Bed Bioreactors. Please note that measurements were done interchangeably between different units during specified time
640 frames.

641 Table 4. Emission rates from different process units and whole plant in 2015.

Investigated wastewater treatment process unit	**Date** (dd/mm)	**CH_4** ($kg\ h^{-1}$) **AV ± SD**	**N_2O** ($kg\ h^{-1}$) **AV ± SD**	**NH_3** ($kg\ h^{-1}$) **AV ± SD**
Sand trap inlet	14/01	3.3±1.5	0.01±0.02	0.05±0.10
	11/03	0.25±0.11	0.01±0.02	0.01±0.02
Primary settlers	13/01	0.64±0.22	0.08±0.05	0.08±0.07
	11/03	0.98±0.46	0.09±0.07	0.04±0.03
Activated sludge reactors	23/06	0.99±0.79	0.060±0.059	0.013±0.011
Nitrifying trickling filters	19/02	n.m.	1.9±1.3	n.m.
	09/03	0.10±0.05	1.8±0.6	0.001±0.001
	23/06	n.m.	4.0±0.8	n.m.
	28&29/08	n.m.	3.2±0.2	n.m.
Post-denitrifying MBBR	19/02	0.008±0.004	0. 08±0.03	<0.002
Secondary settlers	19/02	0.4±0.17	0.18±0.11	0.03±0.02
Ventilation exhaust of thickening and dewatering building	12/01	1.65±0.11	0.041±0.004	0.041±0.010
	17/06	1.74±0.16	0.005±0.001	0.13±0.01
	28/08	3.4±1.4	n.m.	n.m.
Centrifuge room [b]	17/06	0.43±0.01	0.00080±0.00002	0.0043±0.0001
Biosolid stockpiles [c]	13/01	22.5±6.4	0.05±0.06	0.12±0.10
	14/01	20.4±4.5	0.08±0.06	0.17±0.09
	24/06	6.5±2.8 [½14.3±3.5] [a]	0.28±0.15 [1.07±0.38] [a]	0.18±0.11 [0.19±0.09] [a]
	06/07	13.4±2.5 [19.4±5.2] [a]	0.36±0.16 [0.25±0.15] [a]	0.28±0.09 [0.81±0.56] [a]
	28&29/08	9.7±2.5	0.03±0.01	0.12±0.07
Whole plant (plant-integrated measurements)	02/07	n.m.	n.m.	0.4±0.1 [FTIR-SOF]
	28&29/08	28.5 ± 3.1 [FTIR] 33.5 ± 3.0 [CRDS]	4.0 ± 0.8 [FTIR] 6.4 ± 2.1 [CRDS]	0.4±0.2 [FTIR-MTDM]

642 [a] Values in the brackets refer to quantifications during truck loading. [b] Notice that the centrifuge room is placed inside the thickening and dewatering building.
643 FTIR: Fourier Transform InfraRed. CRDS: Cavity Ring-Down Spectroscopy. For results based on inferred flux using STDM or MTDM combined with mass ratios,
644 the given uncertainty corresponds to the combined uncertainty of the STDM/MTDM and the uncertainty in the mass ratio. [c] Note that the sludge digesters were
645 operated in parallel mode January-May, and serial mode June-August. N.m. denotes not measured.
646
647

Table 5. Plant-integrated Emission Factors (EFs).

Gas	Normalization	EF AV ± SD	Method and analytical technology	Average EF
CH_4	kg CH_4 (kg COD $_{influent}$)$^{-1}$ (%)	0.6 ± 0.1	MTDM and FTIR	0.7
		0.7 ± 0.1	MTDM and CRDS	
	kg CH_4 (kg $CH_{4\ production}$) $^{-1}$ (%)	5.4 ± 0.6	MTDM and FTIR	5.9
		6.4 ± 0.6	MTDM and CRDS	
N_2O	kg N_2O-N (kg TN $_{influent}$) $^{-1}$ (%)	0.7 ± 0.1	MTDM and FTIR	0.9
		1.1 ± 0.4	MTDM and CRDS	
	kg N_2O-N (kg TN $_{removed}$) $^{-1}$ (%)	1.0 ± 0.2	MTDM and FTIR	1.2
		1.5 ± 0.5	MTDM and CRDS	
NH_3	kg NH_3-N (kg TN $_{influent}$) $^{-1}$ (%)	0.09 ± 0.04	MTDM and FTIR	0.09
		0.09 ± 0.02	SOF and FTIR	
	kg NH_3-N (kg TN $_{removed}$) $^{-1}$ (%)	0.11 ± 0.05	MTDM and FTIR	0.11
		0.11 ± 0.03	SOF and FTIR	
	kg NH_3-N (kg NH_4^+ $_{influent}$) $^{-1}$ (%)	0.12 ± 0.06	MTDM and FTIR	0.12
		0.12 ± 0.03	SOF and FTIR	
	kg NH_3-N (kg NH_4^+ $_{removed}$) $^{-1}$ (%)	0.15 ± 0.07	MTDM and FTIR	0.15
		0.15 ± 0.04	SOF and FTIR	

AV: average. SD: Standard Deviation. FTIR: Fourier Transform Infrared. CRDS: Cavity Ring-Down Spectroscopy. SOF: Solar Occultation Flux. EFs for CH_4 and NH_3 were normalized to the COD and TN influent content of the wastewater and thus did not consider the COD and TN content in the food waste occasionally fed to the anaerobic digester. Due to the low amounts of food waste fed to the anaerobic digested this would have only minor effect on the EFs (<0.05%).

655 **FIGURES**
656

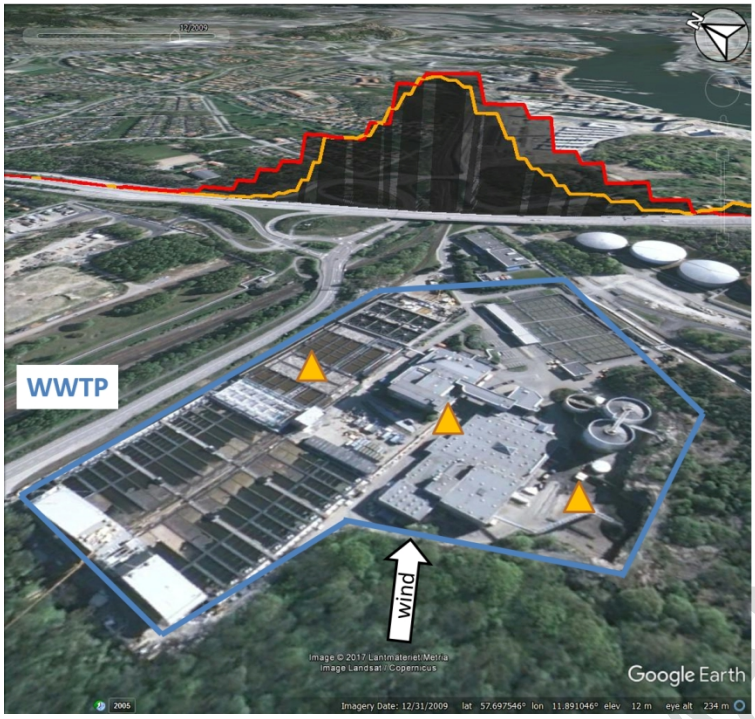

657

658 Figure 1. Downwind methane and acetylene plumes along a road 350 m from the main methane
659 sources measured at 01:15 on 29/08. Yellow triangles mark tracer gas positions. The methane
660 plume is reported in red, while the acetylene plume is depicted with a yellow line. WWTP borders
661 are marked in blue.

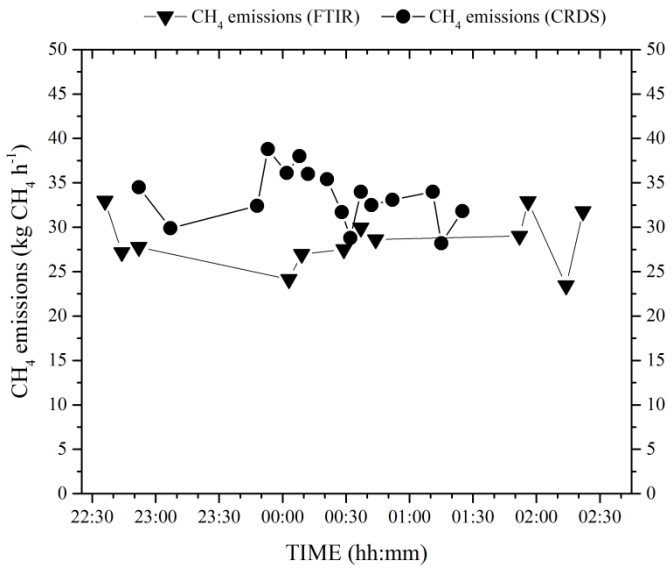

662
663 Figure 2. CH_4 plant-integrated emissions over quantification time (28&29/08) measured with FTIR-
664 MTDM and CRDS-MTDM. FTIR: Fourier Transform InfraRed. CRDS: Cavity Ring-Down
665 Spectroscopy. MTDM: Mobile Tracer Dispersion Method.

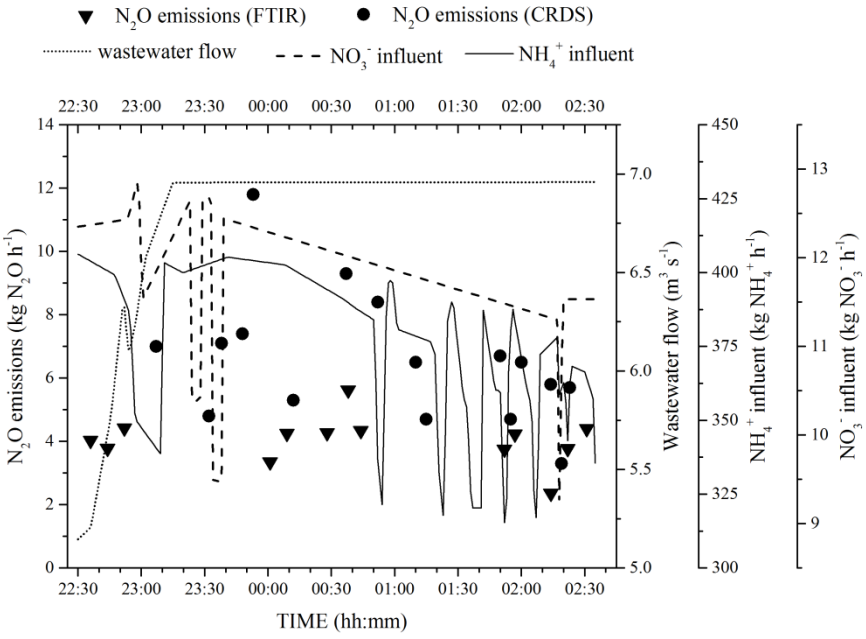

Figure 3. N_2O plant-integrated emissions over quantification time (28&29/08) measured with FTIR-MTDM and CRDS-MTDM. The graph shows the variation in the inlet wastewater flow to the nitrifying trickling filters, as well as the influent of NO_3^- and NH_4^+. FTIR: Fourier Transform InfraRed. CRDS: Cavity Ring-Down Spectroscopy. MTDM: Mobile Tracer Dispersion Method.

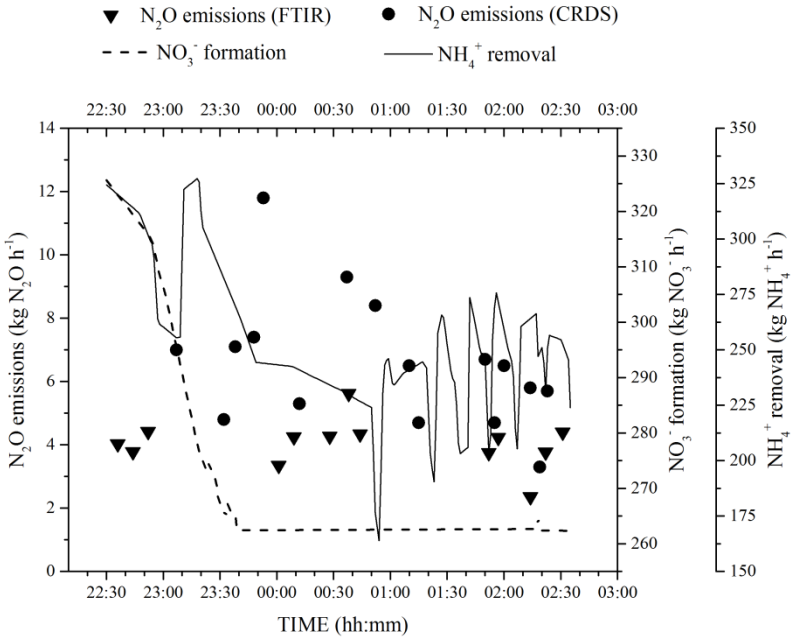

Figure 4. N_2O plant-integrated emissions over quantification time (28&29/08) measured with FTIR-MTDM and CRDS-MTDM. The graph shows NH_4^+ removed and NO_3^- formation based on on-line

measured inlet and outlet concentrations at the nitrifying trickling filters. FTIR: Fourier Transform InfraRed. CRDS: Cavity Ring-Down Spectroscopy. MTDM: Mobile Tracer Dispersion Method.

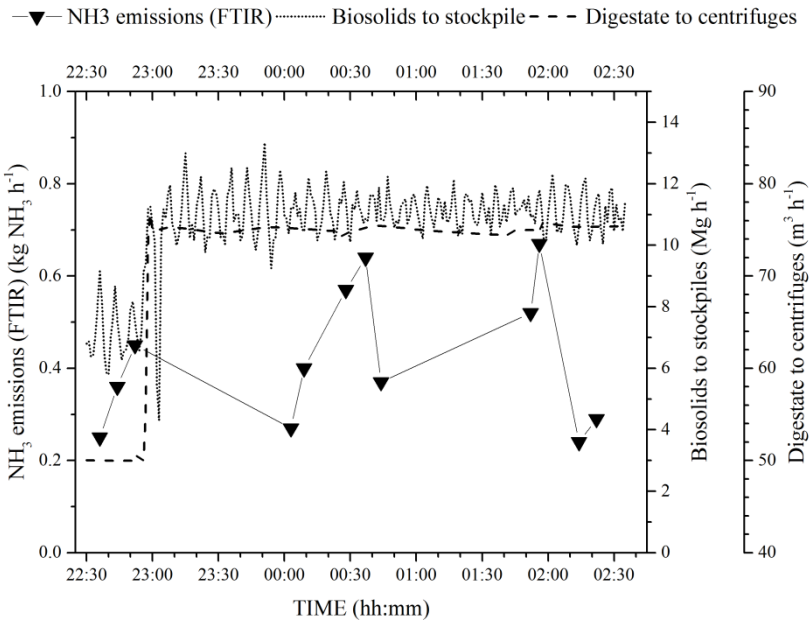

Figure 5. NH_3 plant-integrated emissions over quantification time (28&29/08) measured with FTIR-MTDM. The graph shows the quantity of digestate processed in the centrifuges and the quantity of produced biosolids sent to the stockpiles. FTIR: Fourier Transform InfraRed. CRDS: Cavity Ring-Down Spectroscopy. MTDM: Mobile Tracer Dispersion Method.

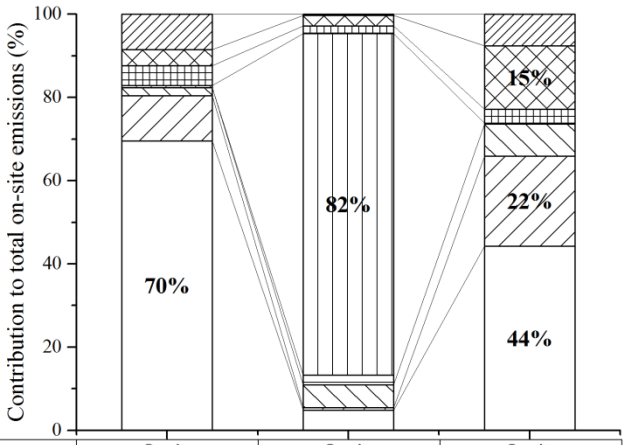

Investigated wastewater treatment process unit	On-site CH_4		On-site N_2O		On-site NH_3	
	Emission rate (kg/h)	Contribution to total (%)	Emission rate (kg/h)	Contribution to total (%)	Emission rate (kg/h)	Contribution to total (%)
Sand trap inlet	1.78	9	0.01	<1	0.03	8
Primary settlers	0.81	4	0.09	3	0.06	15
Activated sludge reactors	0.99	5	0.06	2	0.01	3
Nitrifying trickling filters	0.10	<1	2.73	82	0.001	<1
Post-denitrifying MBBR	0.01	<1	0.08	2	NA	NA
Secondary settlers	0.40	2	0.18	5	0.03	8
Ventilation exhaust of thickening and dewatering building	2.26	11	0.02	1	0.09	22
Biosolid stockpiles	14.50	70	0.16	5	0.17	44
Total on-site quantification	20.85	100	3.32	100	0.39	100

Figure 6. Average contribution of all process units to the total CH_4, N_2O and NH_3 emission quantified from on-site sources.

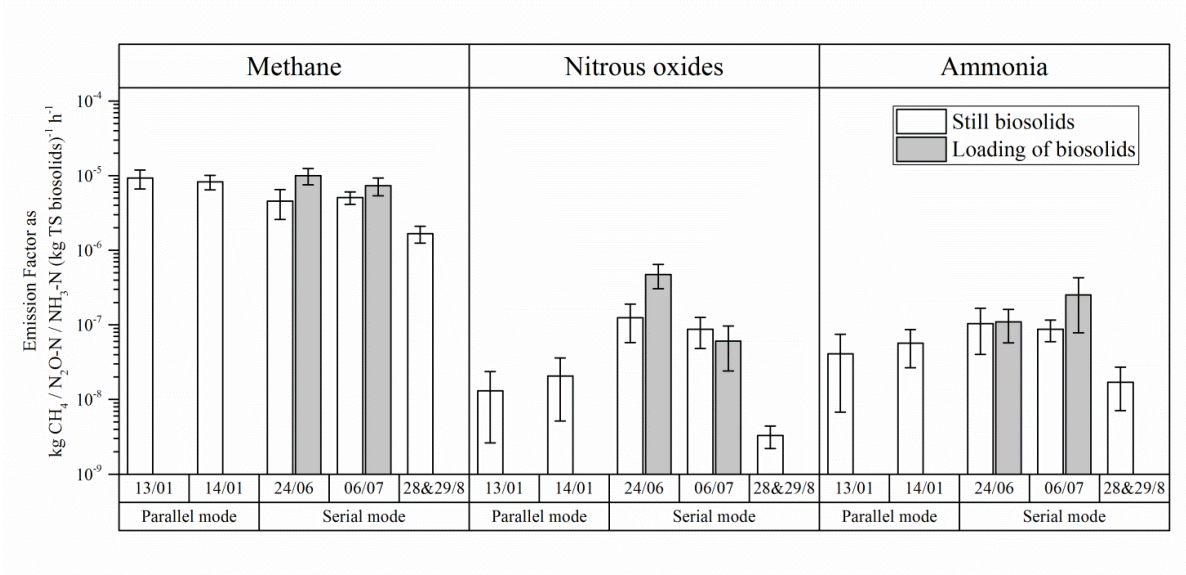

Figure 7. Air emissions from biosolid stockpiles normalized by the amount of stored material. The first two campaigns were performed when digesters were run in parallel, while the remaining were performed when the digesters were run in series. For two measurement campaigns, comparison between still and loading of biosolids is showed. Emission factors (EF) are reported with uncertainty representing the standard deviation of several successful transects. Campaign date is reported as dd/mm since all measurements referred to 2015.

696
697

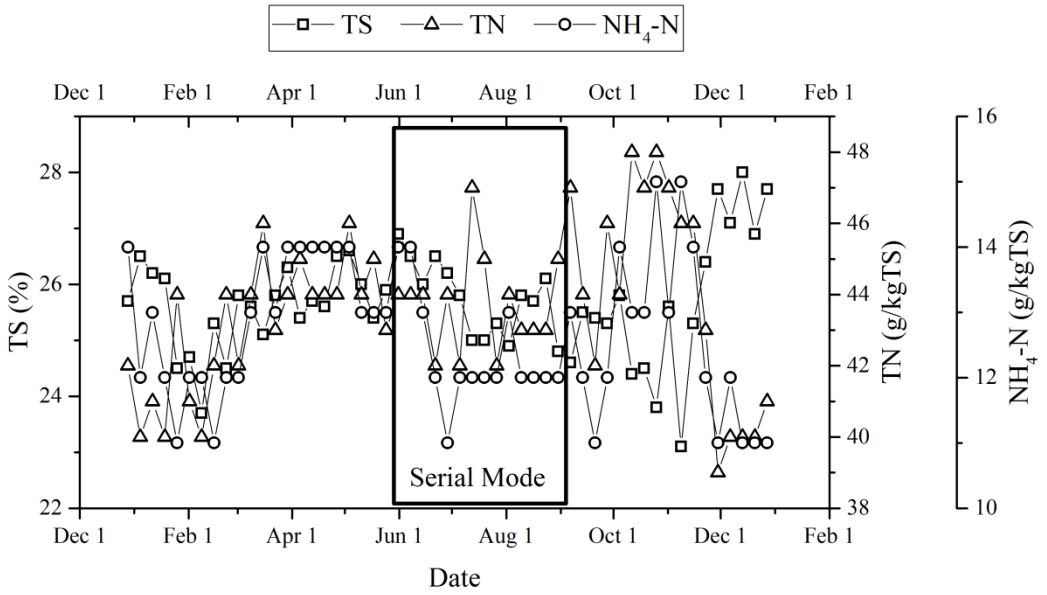

698
699
700 Figure 8. Concentrations of TS, TN and NH_4-N in the produced biosolids in 2015.
701